CHEMISTRY OF MATERIALS

ARTICLE

pubs.acs.org/cm

α-Chalcocite Nanoparticle Synthesis and Stability

Mona Lotfipour, Tony Machani, Daniel P. Rossi, and Katherine E. Plass*

Department of Chemistry, Franklin & Marshall College, Lancaster Pennsylvania 17603, United States

Supporting Information

ABSTRACT: While intensively investigated as a solar light absorber in photovoltaic applications, the use of α-chalcocite (α-Cu_2S) as such has been hindered by its conversion to a copper-deficient, nonstoichiometric phase, djurleite. Here we study this transformation in copper sulfide nanoparticles. We discuss the relative stabilities of α-chalcocite and djurleite as synthesized here, how this influences the conditions for obtaining these phases, and the affect of the reaction conditions on the phase transformation rate. Nanoparticle phases are characterized by powder X-ray diffraction (PXRD) and differential scanning calorimetry (DSC). Size and morphology was characterized by transmission electron microscopy (TEM). Additionally, the α-chalcocite particles were characterized by UV/visible/NIR absorption spectroscopy (UV/vis/NIR) and energy dispersive X-ray spectroscopy (EDS).

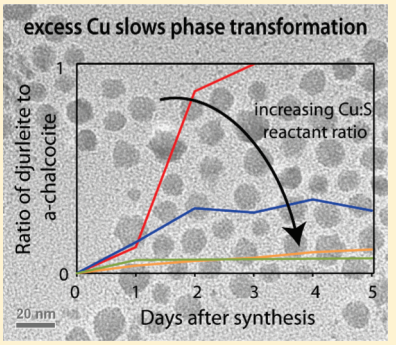

KEYWORDS: chalcocite, djurleite, semiconductor nanoparticles, copper sulfide, phase transformation

INTRODUCTION

Infrared-absorbing nanoparticles are of interest because of their ability to act as efficient absorbers of the solar spectrum, but also for their potential use in IR detectors or plasmonic applications. Toward these ends, nanoparticles of many IR-absorbing materials have been investigated including Cu_4ZnSnS_4 and its solid solutions,[1,2] PbSe,[3] CdTe and CdHgTe,[4] Bi_2S_3,[5] FeS_2,[6,7] and SnS,[8] and GeSe.[9] Of these materials, FeS_2 and Cu_2S stand out as those that combine favorable optical properties with great abundance and low cost.[10] Solar cells using mixtures of β-chalcocite (β-Cu_2S) nanoparticles with CdS[11] nanoparticles or carbon nanotubes[12] have recently been reported, demonstrating the possibility of copper sulfide nanoparticle-based energy conversion devices. Chalcocite, however, has been studied extensively in thin films for use as a solar light absorber,[13−15] but demonstrated stability issues resulting from the phase transformation of chalcocite to a nonstoichiometric phase, djurleite.[13,16,17] Djurleite is a slightly copper-deficient phase existing at Cu/S ratios between 1.94 and 1.97.[18] Nanoparticle morphologies may provide means of altering the relative stabilities of these phases, as has been seen with CdSe[19,20] and Al_2O_3,[21] or they may afford new photovoltaic architectures that reduce the detrimental effects of this transformation.[22] Study of the phase transformations of copper sulfide nanoparticles, therefore, has relevance both to their application in solar energy conversion and to a fundamental understanding of the relationship between morphology and phase behavior.

The synthesis and stability of copper sulfide nanomaterials is complicated by the variability in possible crystalline form and stoichiometry. Copper sulfide exists as two stoichiometric compounds Cu_2S (chalcocite) and CuS (covellite). Chalcocite forms two polymorphs stable at ambient pressure, the low temperature (<103 °C), monoclinic α-form and the more disordered hexagonal β-form.[23] Synthesis of β-chalcocite nanoparticles has been reported on many occasions,[11,12,24−29] while α-chalcocite nanostructure synthesis is only common when they are grown from Cu substrates.[30−35] Otherwise, blue-shifted α-chalcocite particles with band gaps near 2.0 eV[36] have been reported, as have poorly crystalline nanostructures of varying morphologies.[37,38] Copper sulfides also form in a variety of nonstoichiometric phases. Crystalline nanoparticles of anilite ($Cu_{1.75}S$),[39,40] digenite ($Cu_{1.80}S$),[40−45] djurleite ($Cu_{1.97-1.94}S$),[40] and roxbyite (a polymorph of djurleite)[24,46] have been reported. Phase selective copper sulfide nanoparticle synthesis has been carried out by use of different ligands[24] or solvents,[37] as well as by variation of the Cu to S ratio.[41] Burda et al. varied applied potential, pH, and processing conditions to produce covellite, digenite, and djurleite particles.[40]

Review of the literature on α-chalcocite nanoparticles raises an interesting fundamental question regarding the relative stabilities of α-chalcocite and djurleite in thin film versus nanoparticle form. α-Chalcocite transformation to djurleite occurs in both bulk and thin film samples, though it may be so slow as to remain unchanged for many years.[47,48] This transformation is accelerated by oxidation[49] or current.[47] Despite this instability, α-chalcocite can be readily synthesized in thin-films[50−52] and occurs naturally. Djurleite, on the other hand, has been reported as difficult to synthesize purely in bulk using short-term synthesis.[48] In regards to nanoparticles, however, obtaining α-chalcocite nanoparticles rather than djurleite has proven rather difficult, as discussed recently by Burda et al.[40] They synthesized copper sulfide nanoparticles under an extensive range of conditions, but were not able to obtain α-chalcocite. In further support of this, as cited above the literature abounds with reports of

Received: November 3, 2010
Revised: May 16, 2011
Published: May 27, 2011

β-Cu_2S or djurleite, but few of α-chalcocite, suggesting that the relative stability of this phase is reduced for small particles.

Here we examine the relative stabilities of α-chalcocite and djurleite in nanoparticle form by devising conditions under which α-chalcocite nanoparticles do form and comparing these conditions to those that afford djurleite. Furthermore, we examine the transformation of obtained α-chalcocite particles to djurleite, and explore means of slowing α-chalcocite degradation. α-Chalcocite, djurleite, and digenite nanoparticles were obtained by heating copper(II) acetylacetonate ($Cu(acac)_2$) and elemental sulfur in oleylamine, in a synthesis similar to that reported by Zhang, Wu, and Chen,[25] who obtained hexagonal particles of β-chalcocite using $CuCl_2$ starting material. Phase identification was carried out using powder X-ray diffraction and differential scanning calorimetry (DSC). α-Chalcocite nanoparticles were further characterized by ultraviolet/visible/near-infrared (UV/vis/NIR) absorption spectroscopy, transmission electron microscopy (TEM), and energy dispersive X-ray analysis (EDS).

EXPERIMENTAL SECTION

cis-1-Amino-9-octadecene (technical grade), commonly called oleylamine, sulfur (99.98%), and copper(II) acetylacetonate (≥99.99%) were obtained from Sigma-Aldrich. All materials were used as received except for oleylamine, which was dried over molecular sieves.

Typical Reaction. $Cu(acac)_2$ (0.2617 g, 1.0 mmol) and sulfur (0.0160 g, 0.5 mmol) were added to a 3-neck, 50 mL round-bottom flask equipped with a reflux condenser and stir bar. Oleylamine (20 mL, dried over molecular sieves and sparged with argon gas) was added and the reaction vessel was purged with argon gas for 20 min before heating commenced. The reaction was held at 200 °C for 1 h, then 260 °C for 1 h. The reaction was cooled to room temperature and centrifuged at 6000 rpm for 10 min in a 50 mL centrifuge tube. The precipitate was suspended in THF, precipitated with acetone, and then centrifuged to purify the particles. To ensure removal of reactants, the precipitate was again suspended in THF, and the above process was repeated.

Powder X-ray Diffraction (PXRD). PXRD samples were prepared by casting nanoparticle samples onto glass slides from THF or CH_2Cl_2. PXRD experiments were carried out using a PANalytical X'Pert Pro X-ray diffractometer using Cu Kα radiation. The accelerating voltage and current were 45 kV and 40 mA, respectively. Scans were collected from 10 to 75° 2θ. Ten repetitions were summed. The samples were then analyzed using the program PANalytical X'Pert HighScore Plus (Version 2.2e), which allowed comparisons with the ICDD powder X-ray diffraction pattern database (PDF Release 2).

UV/visible/NIR Absorption Spectroscopy. Samples were collected using a Perkin-Elmer Lambda 9/19 spectrometer. Absorbance in the range 1600 to 400 nm was measured at 480 nm/min. Samples were placed in quartz cuvettes intended for use in the near-infrared through visible wavelength regions.

Differential Scanning Calorimetry (DSC). Samples (~10 mg) were placed in Al DSC pans with lids for analysis. A Thermal Analysis DSC Q20 calorimeter was used. Samples and an empty reference pan were heated at 10 °C/min from 40 to 200 °C, allowed to cool, then reheated to observe possible phase transformations, all while under flowing N_2 gas (40.0 L/min).

Transmission Electron Microscopy. Transmission electron microscopy was carried out by solvent-casting samples onto Ni-supported TEM grids with carbon-coating. The microscope was a JEOL 2010F high-resolution TEM with a Schottky field emission gun emitter and a 200 kV accelerating voltage, housed in the Penn Regional Nanotechnology Facility.

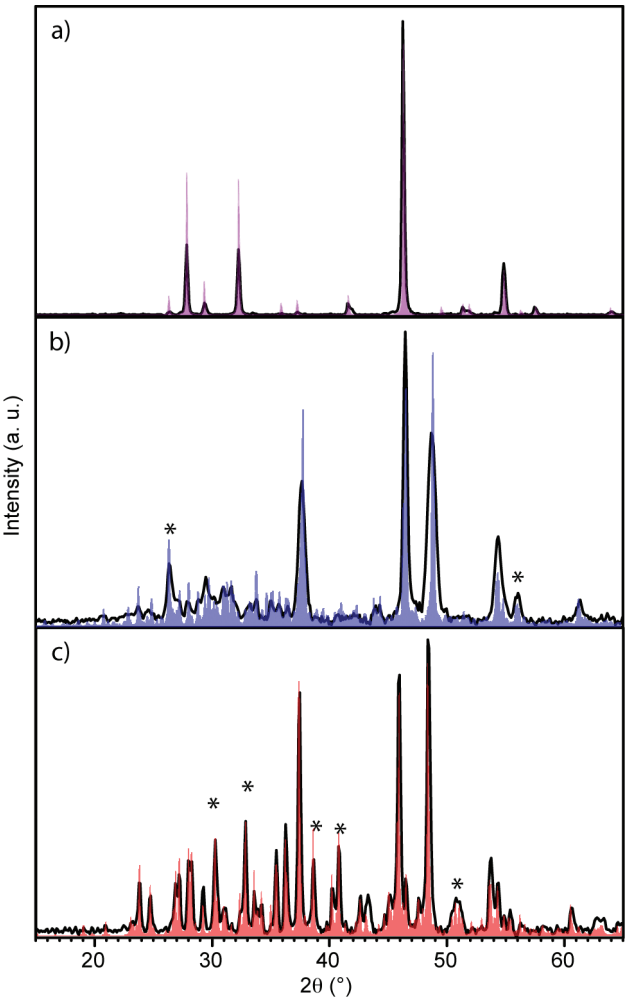

Figure 1. PXRD patterns of obtained copper sulfide nanoparticles synthesized with reactants in Cu/S molar ratios of Cu/S 0.70 (a), 1.3 (b), and 2.16 (c). Matching patterns are overlaid on each (a) cubic digenite [ICDD pattern 047−1748], (b) djurleite [calculated pattern from 100334-ICSD], and (c) α-chalcocite [calculated pattern from 100333-ICSD]. Noted with asterisks are some prominent peaks that distinguish α-chalcocite and djurleite.

Energy Dispersive X-ray Spectroscopy. EDS was carried out using either the transmission electron microscope above equipped with a PGT EDS system or a JEOL 7500F scanning electron microscope equipped with an Oxford Inca Thin Window 10^2 mm EDS. Both instruments are housed in the Penn Regional Nanotechnology Facility.

RESULTS AND DISCUSSION

In the first set of experiments, the ratio of copper and sulfur in the reaction mixture was varied to determine the affect of this parameter on the phase of the resulting nanoparticles. The Cu/S reactant ratio was varied from 0.70:1 to 4.00:1, affording three different copper sulfide phases: digenite, djurleite, and α-chalcocite. Phases were identified using PXRD and confirmed using DSC. Shown in Figure 1 are PXRD patterns obtained from nanoparticles synthesized using Cu/S molar ratios of 2.16:1, 1.3:1, and 0.70:1. As discussed below, digenite was formed consistently at the lowest ratio, while djurleite and α-chalcocite were obtained at ratios of 1.3:1 and 2.16:1, respectively. Pure α-chalcocite synthesis, however, was not consistent, and the

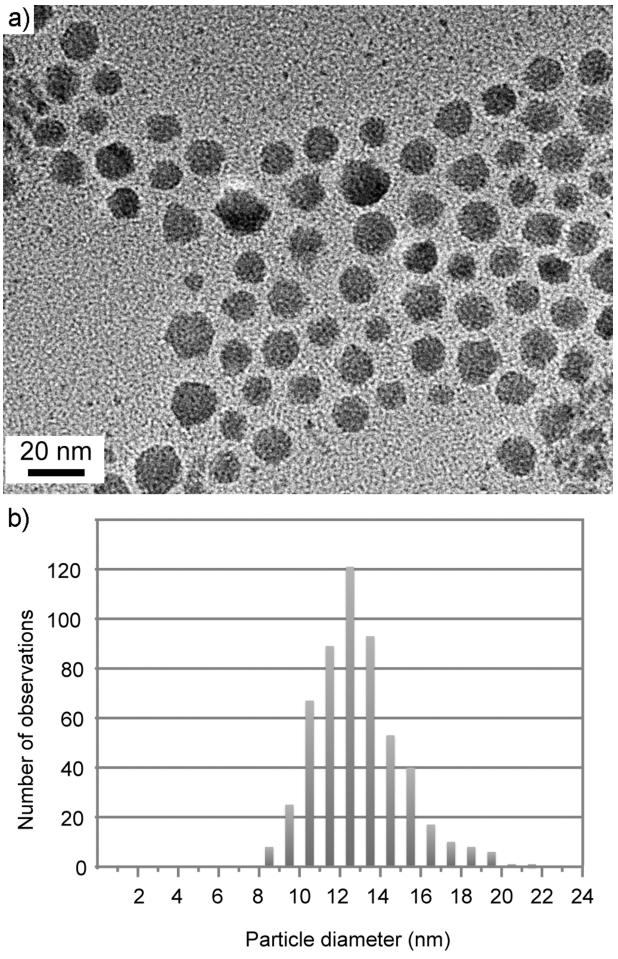

Figure 2. (a) Typical TEM image of α-chalcocite particles obtained by reaction of Cu(II)(acac)2 and S in a 2.11 molar ratio. Particle shapes range from hexagonal to irregular to spherical, with an average particle diameter of 13.0 ± 2.2 nm. (b) Histogram of observed particle diameters showing a range from 8 to 21 nm.

likelihood of obtaining α-chalcocite varied with reactant ratio in a way that suggests it is related to the relative stability of djurleite and α-chalcocite under different conditions.

At the lowest Cu/S molar ratio tested (0.70:1 Cu/S), digenite nanoparticles were reproducibly and reliably obtained. The diffraction pattern of digenite is readily distinguished from that of other copper sulfides. Whereas djurleite and chalcocite (α- and β-forms) are characterized by two prominent peaks near 46 and 48° 2θ, digenite only has one at 46.0° 2θ. This one peak is observed for the lowest Cu/S ratio sample (Figure 1a). The remaining 5 peaks in the PXRD pattern (27.7, 32.0, 54.5, 57.1, and 67.2° 2θ) correspond to those in ICDD pattern [047−1748] for the metastable rhombohedral form of digenite, as distinguished from cubic high digenite.[53] DSC of these particles show a phase transition at 85.7 ± 1.3 °C, as reported for bulk digenite (Supporting Information).[18,48,54] A large excess of sulfur with respect to the Cu/S ratio present in the solid (1.80:1) was required before the digenite phase was observed. Should the copper and sulfur be incorporated into the solid in the ratios they were present in the solution, then covellite (CuS) would be predicted.[18] Much excess sulfur must remain unincorporated, though given the highly reducing nature of oleylamine the concentration of S_2^{-2} is unlikely a limiting factor in formation of the copper sulfide.

The PXRD patterns shown in Figure 1b and 1c demonstrate that α-chalcocite and djurleite were obtained at Cu/S molar ratios of 2.16:1 and 1.3:1, respectively. Both phases were, however, observed over a broad and overlapping reactant ratio range with a frequency that reflects the stabilities of the two phases under different conditions. The PXRD patterns of these two phases are very similar, with many small and overlapping peaks. A more detailed discussion of the PXRD patterns of α-chalcocite and djurleite is presented in the Supporting Information. α-Chalcocite is differentiated from djurleite by the shift of the peak at 46° 2θ, and the presence of peaks at 38.60 and 40.75° 2θ that are much more intense than peaks in djurleite, and by peaks at 30.20 and 32.80° 2θ that are absent in djurleite (Figure 1c). While most of the small peaks in the djurleite pattern are coincident with peaks in α-chalcocite, peaks at 26.20 and 55.75° 2θ are indicative of djurleite formation (Figure 1b).

Obtained α-chalcocite and djurleite particles were further characterized to confirm the phases and determine the size and morphology. DSC measurements of the phase transition temperatures confirmed the phase assignments (Supporting Information). Upon heating, the α-chalcocite particles were observed to transform at 104.4 ± 0.8 °C, in close agreement with the published value of 103.5 °C for transformation into β-chalcocite.[30,48] Djurleite particles exhibited a phase transformation at 92.1 ± 1.3 °C, in agreement with reported behavior.[18,48] The particles (both α-chalcocite and djurleite) were a mixture of shapes including hexagonal and round particles, as well as some irregular shapes (Figure 2a). The particles exhibited sizes ranging from 7 to 21 nm, with an average particle size of 13.0 ± 2.2 nm (Figure 2b). EDS measurements of pure samples (those that have no excess Cu as determined by PXRD) show a Cu/S molar ratio of 2.0 ± 0.2 for α-chalcocite, in agreement with the expected 2:1 ratio.

Both α-chalcocite and djurleite were observed to form over a large and overlapping Cu/S reactant ratio range (between 4.0:1 and 1.15:1), sometimes occurring as mixtures. Djurleite is reliably produced using Cu/S molar ratios of 1.00:1 to 1.15:1, but at ratios between 1.15 and 4.00, there was some likelihood of obtaining either α-chalcocite or djurleite, or a mixture of the two phases. The chances of obtaining pure α-chalcocite were greatest at Cu/S molar ratios between 2.00 and 2.25 (70% of experiments produced pure α-chalcocite while the remainder were α-chalcocite with djurleite impurities). Between 1.15 and 2.00, formation of djurleite was most likely, but α-chalcocite was observed in 25% of experiments. Above 2.25 Cu/S molar ratio, α-chalcocite formed with excess metallic Cu. This inclination to form both phases over such a large range reflects the close thermodynamic competition between the two phases that is altered only subtlety by the reactant ratio, as discussed below. Improved phase selectivity may be achieved by altering synthetic parameters to slow formation of djurleite. An example of this is the use of surfactant to synthesize either β-Cu_2S or roxbyite phase selectively.[24]

The phase behavior in the bulk, while reflecting differences in the reaction conditions and morphology, provides a context for interpreting the phase behavior of these solution-produced nanoparticles and relating it to the relative stabilities of the α-chalcocite and djurleite phases. The phase diagram developed by Potter shows djurleite as the only thermodynamically favored phase at room temperature from Cu/S molar ratios of 1.94 to

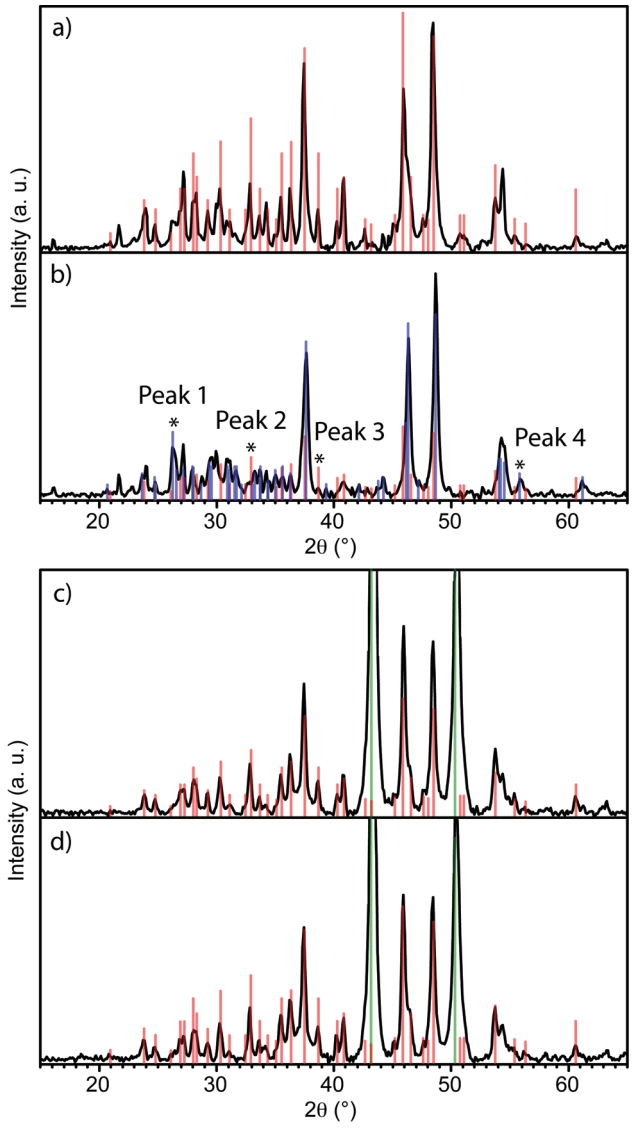

Figure 3. PXRD data for α-chalcocite nanoparticles synthesized with Cu/S molar ratios of 1.99 (a and b) and 3.95 (c and d). Samples are compared immediately after synthesis (a and c) and after storage under ambient conditions (b and d). The lower Cu/S ratio sample transformed to djurleite by day 3 (b), while djurleite is not apparent in the high Cu-content sample by day 7 (d). Patterns of α-chalcocite (red), djurleite (blue), and Cu metal (green) are overlaid on the experimentally obtained patterns.

1.97, with pure α-chalcocite stable in a very narrow range from 1.99 to 2.00.[18] The same diagram shows djurleite and α-chalcocite to coexist from 1.96 to 1.98 Cu/S molar ratio and α-chalcocite to coexist with Cu metal above a 2.00 Cu/S molar ratio. Qualitatively, the observed nanoparticle behavior is in agreement with this phase diagram, in that a transformation from pure djurleite, to a α-chalcocite/djurleite mixture, to α-chalcocite/Cu metal is seen as the Cu/S molar ratio is increased. Other reports deem that djurleite is always more stable than α-chalcocite,[17,55] but that the free energy difference is smallest near the 2:1 Cu/S ratio.[17] This is supported by observations in the bulk that upon heating or applied voltage α-chalcocite slowly transforms to djurleite.[13,47] The observation here that djurleite can be obtained, albeit infrequently, at any Cu/S ratio from 1:00:1 to 4.00:1, supports this proposition. Indeed, this would make pure α-chalcocite formation most likely very close to the 2:1 Cu/S ratio, but would it would still be difficult to completely prevent djurleite formation without some factor affecting the kinetics of formation and slowing djurleite production, as we have observed. Based on reports that inclusion of Zn, Cd, or In improve the stability of α-chalcocite,[56] reactions were run with either Zn or Cd in the forms of $Zn(acac)_2$ and CdO at 10 mol % versus the $Cu(acac)_2$, using Cu/S molar ratios of 1.90 and 2.16. Djurleite was observed in the PXRD pattern with no α-chalcocite formation (Supporting Information). Robust synthesis of α-chalcocite nanostructures has best been demonstrated in the literature by the presence of Cu metal from which the sulfide is grown.[30−35] Another report in which both djurleite and α-chalcocite particles were obtained did not address transformation after synthesis, but did show that djurleite was obtained at shorter reaction times and lower temperatures.[36]

Not only does the reactant ratio affect the likelihood of forming α-chalcocite, but it is also observed to influence the rapidity with which α-chalcocite particles transformed into djurleite. α-Chalcocite samples synthesized using Cu/S reactant molar ratios of 1.99:1 (**1**), 2.09:1, (**2**), 2.23:1 (**3**), and 3.95:1 (**4**), were compared as they aged under ambient conditions. All samples initially contained α-chalcocite, as shown by the characteristic peaks distinguishing α-chalcocite from djurleite at 30.2, 32.8, 38.7, and 40.9° 2θ, but they are not all pure (samples **1** and **4** shown in Figures 3 a and c, respectively). Sample **1**, with the lowest Cu/S reactant ratio, contained djurleite as a minority phase. This is clear from the shoulder at 46.3 on the peak at 45.9° 2θ and the small peak at 26.3° 2θ. Samples **2**, **3**, and **4** did not initially show any evidence of djurleite formation. Within 1 day of synthesis, the PXRD patterns contained those peaks predicted by ICDD pattern [00−023−0961], did not have any of the distinguishing peaks for djurelite, and the ∼46° 2θ peak had the three-pronged shape characteristic of α-chalcocite. Sample **4** contains α-chalcocite and excess metallic Cu (peaks 43.3 and 50.5). Watching the transformation of these species over time reveals that on day 2, djurleite has become the majority phase for sample **1**, and the only apparent phase by day 3 (Figure 3b). Particularly obvious is the change in peak shape and position, as the shoulder of the peak at 45.9° 2θ shifted to a narrow peak at 46.3° 2θ, matching that for djurleite [00−023−0959]. The peaks characteristic of α-chalcocite at 38.7, 32.8, and 30.2° 2θ have shrunk but are still identifiable on day 2, and have disappeared by day 3. Samples **2** and **3** took longer to transform, but do show evidence of djurleite growth. In sample **2**, djurleite had become the majority phase by day 2, but α-chalcocite is still apparent in the sample after 5 days. In sample **3**, djurleite peaks are present on day 2, but on day 5 they still represent a minority phase, with the high intensity α-chalcocite peak at 45.9° 2θ nearly twice as tall as the prominent djurleite peak at 46.3° 2θ. Sample **4**, by comparison, shows no evidence of djurleite formation even after 7 days of storage in ambient conditions (Figure 3d). After two weeks, the sample crystallinity had degraded. Clearly, the presence of excess copper, either in the reactant solution or present in a crystalline or amorphous solid form, helps maintain the equilibrium in favor of α-chalcocite and prevents the lost of Cu atoms that accompanies the transformation from α-chalcocite to djurleite. Calculations by Lukashev et al. conclude α-chalcocite is thermodynamically unstable with respect to djurleite even when in equilibrium with Cu,[55] but clearly the presence of copper slows the transformation of α-chalcocite to

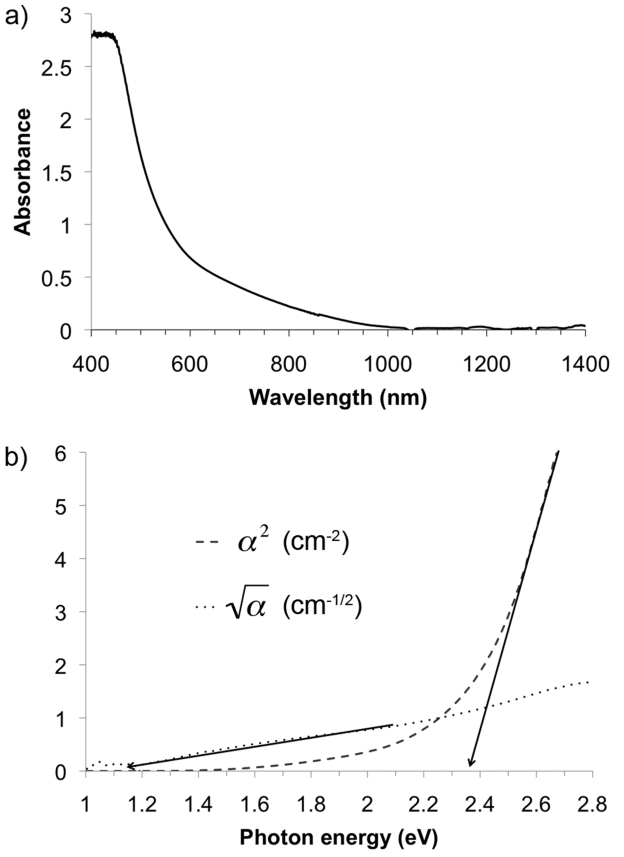

Figure 4. (a) UV/vis/NIR absorbance spectrum of α-chalcocite nanoparticles suspended in oleylamine and b) the square root of the absorptivity (dots) and the square of the absorptivity (dashes) plotted versus the photon energy. Note the onset absorbance near 1150 nm due the to lowest indirect band gap of 1.11 ± 0.01 eV (the *x*-intercept of the straight line fitted to the square-root of the absorptivity) and the increased absorbance starting around 550 nm due to the direct band gap of 2.4 eV.

djurleite. This may explain why α-chalcocite nanostructures are often obtained from Cu substrates, but by so few other routes.[34]

The reduced stability of α-chalcocite in nanoparticle form with respect to the bulk or thin films could be explained by the increased surface area. This increased surface area could both allow for improved diffusion of Cu ion out of the crystal and could increase surface oxidation, which has been linked to,[40] but does not necessarily result in,[13] djurleite formation. Surface energy effects such as those that stabilize wurtzite CdSe nanoparticles with respect to transformation to the rock salt phase[20] are unlikely to play a role in this situation because of the similarity in the crystal structures of α-chalcocite and djurleite. Both have nearly identical, hexagonal sulfide frameworks and differ primarily in the superstructure of the copper cations. Likely, transformation of α-chalcocite to djurleite occurs more readily because the increased surface area increases the ease of with which copper ions escape the crystal. This surface-area-based argument is supported by the observations that the obtained particles are not so small that either the optical or phase transformation behavior deviates from the bulk. At 13 nm in diameter, a lack of quantum confinement would be unsurprising (these are considerable larger than the 3 and 5.5 nm α-chalcocite particles that exhibit blue-shifted onset absorbances[36]) and is not observed. The lack of quantum confinement is confirmed by the UV/vis/NIR absorption spectroscopy (Figure 4), which shows that the obtained α-chalcocite has an indirect band gap of 1.11 ± 0.01 eV, in agreement with reported band gaps of 1.2[57] and 1.1 eV.[49,58] Furthermore, the similarity in phase transformation temperature between the bulk and nanoparticle forms, as discussed above, confirms that the enthalpy of transformation is unchanged, unlike in the reduced melting points of gold particles, for example.[59] These parallels between the bulk and 13 nm diameter nanoparticles suggests that the crystal structure itself is not further destabilized in comparison with the bulk, but that the kinetics of degradation may be increased.

Surface oxidation may also play a role in the reduced stability of α-chalcocite in nanoparticle form with respect to the bulk or thin films. The transformation from α-chalcocite to djurleite is aided by surface oxidation,[16] though it is not dependent upon it. For example, transformation has been observed to occur during TEM imaging in vacuum because of reduction by the electron beam[60] and chalcocite can oxidize without forming djurleite.[13] Metal sulfide nanoparticles have been shown to be less stable toward oxidation than bulk materials[61] and size can affect the mechanism for oxidation, causing sulfite or sulfate production, for example.[62] Synthesis here was carried out under anaerobic conditions, so the difficulty in synthesizing α-chalcocite is still best ascribed to an increased rate of transformation to djurleite due to rapid Cu diffusion from the crystal. In the experiment here in which transformation from α-chalcocite to djurleite was monitored by PXRD, samples were stored under ambient, oxygen-containing conditions. Oxidation very likely plays a role in the transformation of α-chalcocite to djurleite observed. For comparison, β-chalcocite nanoparticles that provided stable photovoltaics performance for months under anaerobic conditions[11] were reported to show the long-wavelength absorbance associated with $Cu_{2-x}S$ after air exposure.[40] Formation of copper oxide species shifts the stoichiometry toward ratios that favor djurleite formation, speeding this transformation.

The role of excess copper in slowing transformation to djurleite is in accordance with Le Châtelier's principle, regardless of whether the transformation occurs in ambient or anaerobic conditions. Copper metal is a product of the degradation, so adding copper shifts the equilibrium in favor of α-chalcocite, though calculations suggest that α-chalcocite is still thermodynamically less favorable than djurleite under these conditions.[55] While excess copper can slow degradation to djurleite, it is unlikely to be a successful long-term strategy for slowing degradation in photovoltaics. Using a mixture of chalcocite and copper as a solar light absorber would be untenable due to the high reflectivity of copper and the interference of the metal with electron transfer pathways, such was observed in thin film Cu_2S cells.[13] Elucidation of the role of copper in preventing djurleite formation, coupled with the knowledge that the large surface area of nanoparticles encourages transformation of α-chalcocite to djurleite suggests, perhaps, that routes to slowing or stopping this transformation could be found by addition of dopants or formation of solid solutions that could hinder copper ion movement, or by appropriate surface chemistry treatment.

CONCLUSIONS

Here α-chalcocite nanoparticles were synthesized, and were found to be unstable with respect to djurelite formation to a greater extent than observed in the thin film or bulk morphologies.

This instability affects the synthetic conditions under which α-chalcocite particles are obtained and the frequency with which they form concurrent with djurleite. The addition of excess copper slows the rate of transformation, which suggests means of controlling this undesirable phase behavior.

■ ASSOCIATED CONTENT

Supporting Information. DSC graphs, a description of how to distinguish the PXRD patterns of α-chalcocite and djurleite, PXRD patterns showing the affect of Zn on the obtained copper sulfide phase, the PXRD peak intensity ratios plotted versus storage time, TEM image of an α-Cu_2S sample with excess Cu, and a detailed description of the UV/visible/NIR absorption of α-chalcocite. This material is available free of charge via the Internet at http://pubs.acs.org.

■ AUTHOR INFORMATION

Corresponding Author
*E-mail: kplass@fandm.edu.

■ ACKNOWLEDGMENT

The authors thank Franklin & Marshall College for start-up funds, for student grants, and for student support via the Hackman Summer Scholars Program, as well as the Henry and Camille Dreyfus Foundation for a New Faculty Startup Award and Research Corporation for a Cottrell College Science Award. TEM and SEM measurements were made possible through the Penn Regional Nanotechnology Facility, Materials Research Facilities Network of the MRSEC Program of the National Science Foundation under award #DMR05-20020, and the assistance of Dr. Douglas Yates and Dr. Lolita Rotkina.

■ REFERENCES

(1) Dai, P. C.; Shen, X. N.; Lin, Z. J.; Feng, Z. Y.; Xu, H.; Zhan, J. H. *Chem. Commun.* **2010**, *46*, 5749–5751.
(2) Riha, S. C.; Parkinson, B. A.; Prieto, A. L. *J. Am. Chem. Soc.* **2009**, *131*, 12054–12055.
(3) Koleilat, G. I.; Levina, L.; Shukla, H.; Myrskog, S. H.; Hinds, S.; Pattantyus-Abraham, A. G.; Sargent, E. H. *ACS Nano* **2008**, *2*, 833–840.
(4) Yang, Z. S.; Chang, H. T. *Sol. Energy Mater. Sol. Cells* **2010**, *94*, 2046–2051.
(5) Vogel, R.; Hoyer, P.; Weller, H. *J. Phys. Chem.* **1994**, *98*, 3183–3188.
(6) Hu, Y.; Zheng, Z.; Jia, H. M.; Tang, Y. W.; Zhang, L. Z. *J. Phys. Chem. C* **2008**, *112*, 13037–13042.
(7) Wadia, C.; Wu, Y.; Gul, S.; Volkman, S. K.; Guo, J. H.; Alivisatos, A. P. *Chem. Mater.* **2009**, *21*, 2568–2570.
(8) Baumgardner, W. J.; Choi, J. J.; Lim, Y. F.; Hanrath, T. *J. Am. Chem. Soc.* **2010**, *132*, 9519–9521.
(9) Vaughn, D. D.; Patel, R. J.; Hickner, M. A.; Schaak, R. E. *J. Am. Chem. Soc.* **2010**, *132*, 15170–15172.
(10) Wadia, C.; Alivisatos, A. P.; Kammen, D. M. *Environ. Sci. Technol.* **2009**, *43*, 2072–2077.
(11) Wu, Y.; Wadia, C.; Ma, W. L.; Sadtler, B.; Alivisatos, A. P. *Nano Lett.* **2008**, *8*, 2551–2555.
(12) Lee, H.; Yoon, S. W.; Kim, E. J.; Park, J. *Nano Lett.* **2007**, *7*, 778–784.
(13) Chopra, K. L.; Das, S. R. *Thin Film Solar Cells*; Plenum Press: New York, 1983.
(14) Norian, K. H.; Hall, R. B. *Thin Solid Films* **1982**, *88*, 55–66.
(15) Bragagnolo, J. A.; Barnett, A. M.; Phillips, J. E.; Hall, R. B.; Rothwarf, A.; Meakin, J. D. *IEEE Trans. Electron Devices* **1980**, *27*, 645–651.
(16) Aldhafiri, A. M.; Russell, G. J.; Woods, J. *Semicond. Sci. Technol.* **1992**, *7*, 1052–1057.
(17) Putnis, A. *Philos. Mag.* **1976**, *34*, 1083–1086.
(18) Potter, R. W. *Econ. Geol.* **1977**, *72*, 1524–1542.
(19) Chen, C. C.; Herhold, A. B.; Johnson, C. S.; Alivisatos, A. P. *Science* **1997**, *276*, 398–401.
(20) Tolbert, S. H.; Alivisatos, A. P. *Science* **1994**, *265*, 373–376.
(21) McHale, J. M.; Auroux, A.; Perrotta, A. J.; Navrotsky, A. *Science* **1997**, *277*, 788–791.
(22) Kayes, B. M.; Atwater, H. A.; Lewis, N. S. *J. Appl. Phys.* **2005**, *97*, 114302.
(23) Evans, H. T. *Science* **1979**, *203*, 356–358.
(24) Lim, W. P.; Wong, C. T.; Ang, S. L.; Low, H. Y.; Chin, W. S. *Chem. Mater.* **2006**, *18*, 6170–6177.
(25) Zhang, H. T.; Wu, G.; Chen, X. H. *Langmuir* **2005**, *21*, 4281–4282.
(26) Zhuang, Z. B.; Peng, Q.; Zhang, B.; Li, Y. D. *J. Am. Chem. Soc.* **2008**, *130*, 10482–10483.
(27) Larsen, T. H.; Sigman, M.; Ghezelbash, A.; Doty, R. C.; Korgel, B. A. *J. Am. Chem. Soc.* **2003**, *125*, 5638–5639.
(28) Chen, L.; Chen, Y. B.; Wu, L. M. *J. Am. Chem. Soc.* **2004**, *126*, 16334–16335.
(29) Sigman, M. B.; Ghezelbash, A.; Hanrath, T.; Saunders, A. E.; Lee, F.; Korgel, B. A. *J. Am. Chem. Soc.* **2003**, *125*, 16050–16057.
(30) Wang, S. H.; Guo, L.; Wen, X. G.; Yang, S. H.; Zhao, J.; Liu, J.; Wu, Z. H. *Mater. Chem. Phys.* **2002**, *75*, 32–38.
(31) Gorai, S.; Ganguli, D.; Chaudhuri, S. *Mater. Chem. Phys.* **2004**, *88*, 383–387.
(32) Lai, C. X.; Wu, Q. B.; Chen, J.; Wen, L. S.; Ren, S. *Nanotechnology* **2010**, *21*, 215602.
(33) Wang, S. H.; Yang, S. H. *Chem. Phys. Lett.* **2000**, *322*, 567–571.
(34) Wang, S. H.; Yang, S. H. *Adv. Mater. Opt. Electron.* **2000**, *10*, 39–45.
(35) Zhao, S. Z.; Han, G. Y.; Li, M. Y. *Mater. Chem. Phys.* **2010**, *120*, 431–437.
(36) Chen, Y. B.; Chen, L.; Wu, L. M. *Chem.—Eur. J.* **2008**, *14*, 11069–11075.
(37) Gorai, S.; Ganguli, D.; Chaudhuri, S. *Cryst. Growth Des.* **2005**, *5*, 875–877.
(38) As noted by Evans[23] and Burda et al.,[40] materials reported as chalcocite are often better matched to djurleite.
(39) Liufu, S. C.; Chen, L. D.; Yao, Q.; Huang, F. Q. *J. Phys. Chem. C* **2008**, *112*, 12085–12088.
(40) Zhao, Y. X.; Pan, H. C.; Lou, Y. B.; Qiu, X. F.; Zhu, J. J.; Burda, C. *J. Am. Chem. Soc.* **2009**, *131*, 4253–4261.
(41) Ghezelbash, A.; Korgel, B. A. *Langmuir* **2005**, *21*, 9451–9456.
(42) Lou, W. J.; Chen, M.; Wang, X. B.; Liu, W. M. *J. Phys. Chem. C* **2007**, *111*, 9658–9663.
(43) Zhang, H.; Zhang, Y. Q.; Yu, J. X.; Yang, D. R. *J. Phys. Chem. C* **2008**, *112*, 13390–13394.
(44) Lu, Q. Y.; Gao, F.; Zhao, D. Y. *Nano Lett.* **2002**, *2*, 725–728.
(45) Lou, Y. B.; Samia, A. C. S.; Cowen, J.; Banger, K.; Chen, X. B.; Lee, H.; Burda, C. *Phys. Chem. Chem. Phys.* **2003**, *5*, 1091–1095.
(46) Lim, W. P.; Low, H. Y.; Chin, W. S. *Cryst. Growth Des.* **2007**, *7*, 2429–2435.
(47) Putnis, A. *Am. Mineral.* **1977**, *62*, 107–114.
(48) Roseboom, E. H. *Econ. Geol.* **1966**, *61*, 641–672.
(49) Partain, L. D.; McLeod, P. S.; Duisman, J. A.; Peterson, T. M.; Sawyer, D. E.; Dean, C. S. *J. Appl. Phys.* **1983**, *54*, 6708–6720.
(50) Schneider, S.; Ireland, J. R.; Hersam, M. C.; Marks, T. J. *Chem. Mater.* **2007**, *19*, 2780–2785.
(51) Schneider, S.; Yang, Y.; Marks, T. J. *Chem. Mater.* **2005**, *17*, 4286–4288.
(52) Savelli, M.; Bougnot, J. In *Solar Energy Conversion: Solid-State Physics Aspects*; Seraphin, B. O., Ed.; Springer-Verlag: New York, 1979, p 216−250.

(53) Morimoto, N.; Kullerud, G. *Am. Mineral.* **1963**, *48*, 110–123.
(54) Grguric, B. A.; Harrison, R. J.; Putnis, A. *Mineral. Mag.* **2000**, *64*, 213–231.
(55) Lukashev, P.; Lambrecht, W. R. L.; Kotani, T.; van Schilfgaarde, M. *Phys. Rev. B* **2007**, *76*, 195202.
(56) Okamoto, K.; Kawai, S. *Jpn. J. Appl. Phys.* **1973**, *12*, 1130–1138.
(57) Liu, G. M.; Schulmeyer, T.; Brotz, J.; Klein, A.; Jaegermann, W. *Thin Solid Films* **2003**, *431*, 477–482.
(58) Xu, Y.; Schoonen, M. A. A. *Am. Mineral.* **2000**, *85*, 543–556.
(59) Sambles, J. R. *Proc. R. Soc. London, Ser. A* **1971**, *324*, 339–351.
(60) Posfai, M.; Buseck, P. R. *Am. Mineral.* **1994**, *79*, 308–315.
(61) Sykora, M.; Koposov, A. Y.; McGuire, J. A.; Schulze, R. K.; Tretiak, O.; Pietryga, J. M.; Klimov, V. I. *ACS Nano* **2010**, *4*, 2021–2034.
(62) Tang, J.; Brzozowski, L.; Barkhouse, D. A. R.; Wang, X. H.; Debnath, R.; Wolowiec, R.; Palmiano, E.; Levina, L.; Pattantyus-Abraham, A. G.; Jamakosmanovic, D.; Sargent, E. H. *ACS Nano* **2010**, *4*, 869–878.